Review

DOI: 10.5582/bst.2026.01032

Characteristics and management of constitutional indocyanine green excretory defect

Jiaao Wang, Ziqi Hou, Jun Ji, Ding Hu, Changlong Wei, Zhihong Zhang, Yuanzhi Zhou, Haichuan Wang*, Jiwei Huang*

Division of Liver Surgery, Department of General Surgery, West China Hospital, Sichuan University, Chengdu, China.

SUMMARY: Indocyanine green (ICG) test is a popular and widely implied assessment of hepatic functional reserve (HFR) due to its safety and efficiency. However, as the application of ICG expanded, an exceedingly rare disorder, the constitutional ICG excretory defect (CIED), gradually emerged. CIED is considered as a harmless dye excretory defect, which features remarkable ICG plasma retention (plasma ICG 15-min retention rate is higher than 50%) without any severe liver impairments. Previous investigations revealed that it has no particular symptoms and it is not a contraindication of surgical treatments. The deficiency of the organic anion transporting polypeptide 1B3 is affirmed to be the underlying cause of CIED. It is of great significance to identify this disorder from other reasons elevating ICG-R15 and provide such patients with effective and safe treatments. The utility of ^{99m}Tc-GSA liver scintigraphy, Child-Pugh and ALBI scores, and liver biopsy in identification and supplementary HFR assessment in CIED has been affirmed. Moreover, other methods based on radioactive tracers, serum biomarkers and imaging examinations have potential. Based on existing evidence, we proposed a clinical strategy that prioritizes ALBI and Child-Pugh scores, as well as imaging examinations, such as computerized tomography and ultrasound examinations, for the initial identification of CIED. Thereafter, ^{99m}Tc-GSA liver scintigraphy or biopsy is used to verify CIED and assess HFR. In conclusion, we comprehensively reviewed the characteristics, mechanisms and coping strategies of CIED, aiming to provide updated insights of this disorder.

Keywords: indocyanine green, organic anion transport, liver function test, liver surgery, liver disease

1. Introduction

Hepatic functional reserve (HFR) represents the liver's residual functional capacity to maintain physiological demands following injury or surgical resection, primarily determined by the quantity of viable hepatocytes and the integrity of hepatic microstructure (*1*). As a critical preoperative assessment in hepatic surgery, accurate HFR evaluation serves dual purposes: it identifies surgical candidates while guiding optimal surgical strategies to achieve complete lesion resection while minimizing postoperative complications, particularly post hepatectomy liver failure (PHLF) (*2*). This balance between radical tumor removal and preservation of sufficient functional liver tissue underscores the essential role of HFR assessment in modern hepatobiliary surgery.

So far, plenty of methods have been developed to assess HFR accurately, including laboratory tests, score systems, liver specific biomarkers, radioactive tracers, *etc*. (*1,3-7*). Among these, indocyanine green (ICG) is one of the most common methods due to its safety and accuracy in preoperative HFR evaluation (*5,8*). ICG was firstly introduced as a supplantation of bromosulphophthalein (BSP) because BSP occasionally causes severe complications. BSP is also taken up by the liver and undergoes enterohepatic circulation, leading to less accurate test results compared with ICG (*9,10*). The most used parameter is the retention rate of ICG at 15 minutes (ICG-R15), which was first introduced by Makuuchi *et al*. (*11*). However, in the past few decades an intriguing category of cases was encountered, which features extremely high blood retention rates of ICG (ICG-R15 usually higher than 50%) with other liver function being normal or only mildly abnormal. Such cases were defined as constitutional ICG excretory defect (CIED) (Figure 1) (*12-14*).

Following intravenous administration, ICG directly binds to plasma proteins and is transported to hepatic sinusoids by blood flow (*10,15*). Then the ICG, existing as an organic anion, is absorbed by organic anion transporters over the basolateral membrane, passes through the hepatic cell without metabolic changes

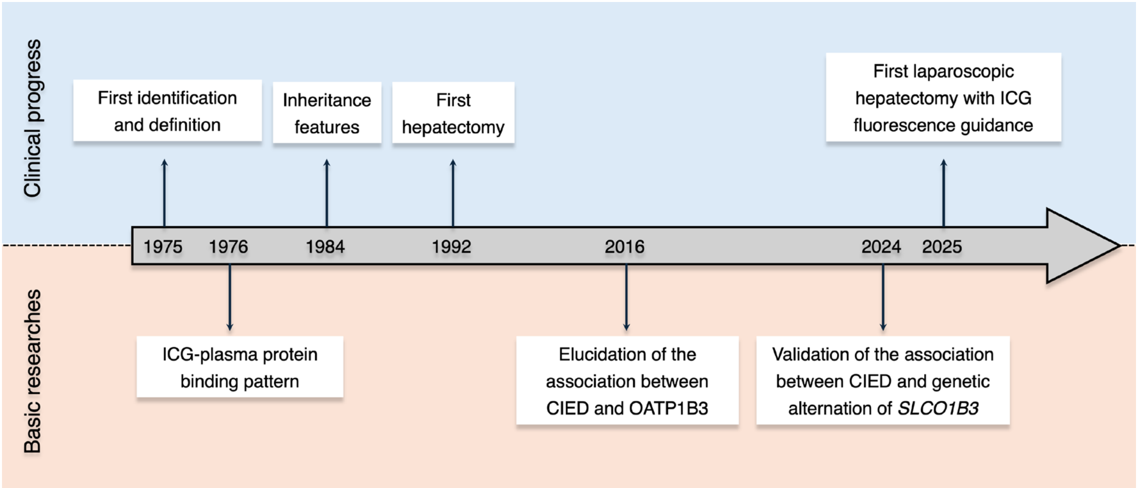

Figure 1. Milestones of CIED research in clinical and basic aspects.

and is excreted with bile acid through canaliculi membranes (*15,16*). This efficient hepatic clearance can be disrupted by multiple pathophysiological factors, such as architectural distortion in fibrosis/cirrhosis, impairing sinusoidal perfusion and hepatocyte function, hemodynamic alterations, competitive inhibition from hyperbilirubinemia and genetic or acquired variations in transporter expression (*15-20*). These mechanisms collectively contribute to the spectrum of observed ICG retention abnormalities in clinical practice.

Despite its rarity, accurate identification of CIED carries significant clinical implications, necessitating both reliable diagnostic criteria and validated alternative HFR assessment strategies for affected patients. Our systematic literature review (search terms: "indocyanine green" and "excretory defect" or "plasma retention" in PubMed and Google Scholar), initially identified 30 relevant publications. After excluding publications without specific cases and unavailable ones, 22 of the most relevant publications were reviewed. In this paper, we first reviewed the typical cases and studies of CIED and then concluded the features. Thereafter, studies related to the pathogenicity of CIED were thoroughly discussed. The last part focused on the examinations with differentiation significance and potential substitute HFR assessments for such patients. The findings aim to guide clinical decision-making while highlighting knowledge gaps requiring further investigation.

2. Epidemiology and clinical manifestations

Due to the rarity of CIED, there is lack of epidemiology investigations on large populations. Till now, all of CIED-related publications were reported in Japan (*12,13,21-39*) and China (*40*). Few reports of CIED in other countries were published. This might be attributed to the application of ICG mainly at these specific areas (*2*). Additionally, there has been no exact evidence to demonstrate that CIED is significantly affected by age, sex or race.

Namihisa *et al.* first reported 4 typical CIED cases. Relevant basic information is listed in Table 1. The laboratory tests and physical examinations revealed no abnormal findings. The only abnormal results were extremely high ICG-R15, which were all higher than 69%. The plasma ICG disappearance curve of 4 cases revealed there was a significant delay in the initial stage, and a step-form transitional delay in 15-25 minutes after injection. The ICG plasma disappearance rate also remarkably decreased, ranging from 0.017 to 0.025, significantly lower than normal limit of 0.15 (*41*). The following analysis revealed the transfer rate of ICG from plasma to liver was markedly decreased, with the normal transfer rate of ICG from liver to bile and liver back to plasma. Neither structural change nor heterogeneous cell infiltration were observed in liver biopsies of 4 cases. Additionally, the electron-microscopy found that there were increases of "lipofuscin-like" lysosomes in the hepatocyte and reticulum fiber in Disse's space, paracrystalline-like arrangement of mitochondria, and fragmentation of rough-surfaced endoplasmic reticulum (*12*). This study generally concluded the clinical characters and ICG kinetics features of CIED. The 2 stages delay in the plasma disappearance curve and significantly decreased ICG clearance rate (KICG) based on normal liver laboratory and histology tests were suggested as features of CIED (*12*). A further study by Adachi *et al.* supported previous findings. Also, the analysis of ICG plasma protein binding pattern revealed that there was no difference between cases and normal people, providing more evidence suggesting that the plasma retention of ICG was caused by limited uptake function of hepatocytes (*21*). Subsequently, other similar studies were conducted, with consistent conclusions (*22,23,25*).

Moreover, Taketazu *et al.* reported a case of CIED with malaria and hereditary elliptocytosis, which is another rare congenital disorder featuring elliptical-

Table 1. A summary of case reports of CIED

Author	Time	Report ccontent	Case number	Age & Gender	ICG-R15%	Disease	*Ref.*
Namihisa, *et al.*	1975	High retention of ICG test and normal retention of BSP test	4	52F	70.5	cholecystitis	(*12*)
				32M	78.4	duodenal ulcer	
				28F	70.2	healthy	
				60M	69.4	colon carcinoma	
Adachi, *et al.*	1976	Serum protein binding pattern in high ICG retention patients	5	28M	75.7	Gilbert's Syndrome	(*21*)
				24M	74.1	Gilbert's Syndrome	
				65M	82.8	diabetes mellitus and liver cirrhosis	
				37M	88.3	chronic persistent hepatitis with fatty infiltration	
				19M	84.9	Lung tuberculosis	
Okuda, *et al.*	1976	High retention of ICG test and normal results of BSP test	5	22M	67.3	Gilbert's Syndrome	(*13*)
				34M	68.4	Gilbert's Syndrome	
				25M	88.2	chronic cervical lymphadenitis	
				35F	76.0	acute HBsAg-negative hepatitis	
				70M	64.0	prostate carcinoma	
Taketazu, *et al.*	1984	CIED patients with hereditary elliptocytosis	1	28F	94.0	malaise and elliptocytosis	(*23*)
Gotoh, *et al.*	1992	Hepatectomy in biliary cystadenocarcinoma with CIED	1	45F	99.8	biliary cystadenocarcinoma and Hepatitis B	(*24*)
Ikejima, *et al.*	1993	Chronic persistent hepatitis with high retention of ICG and BSP without hyperbilirubinemia	1	51M	70.0	HBV carrier	(*25*)
Hanazaki, *et al.*	2000	Hepatectomy in cavernous hemangioma patient with CIED	1	47F	59.8	cavernous hemangioma	(*27*)
Yamanaka, *et al.*	2001	Hepatectomy in HCC patient with chronic HBV, HCV and CIED	1	61M	72.0	HCC with chronic HBV, HCV	(*28*)
Kadono, *et al.*	2006	Effectiveness of ^{99m}Tc-GSA in preoperative evaluating patient with CIED and choledocholithiasis, receiving hepatectomy	1	78F	79.3	biliary cystadenocarcinoma	(*29*)
Maeda, *et al.*	2007	Hepatectomy in HCC patient with CIED	1	69F	83.5	HCC	(*30*)
Aoki, *et al.*	2013	Hepatectomy in HCC patient with Dubin–Johnson syndrome and CIED	1	77M	77.1	HCC with Dubin-Johnson syndrome	(*31*)
Imada, *et al.*	2016	Association between CIED and the expression of OATPs and NTCPs	1	81M	79.1	HCC	(*32*)
Nakatake, *et al.*	2018	Hepatectomy in a case of HCC with CIED	1	83M	76.2	HCC	(*34*)
Masuoka, *et al.*	2020	Effectiveness of gadoxetic acid-enhanced MRI in CIED	3	58M	83.0	HCC with HBV	(*37*)
				70M	68.0	CRLM after right hemicolectomy	
				69M	73.0	hilar cholangiocarcinoma	
Liu, *et al.*	2021	Hepatectomy in HCC patient with constitutional ICG excretory defect	1	68M	82.9	HCC	(*40*)
Morikawa, *et al.*	2025	Laparoscopic hepatectomy using ICG fluorescence staining in HCC patient with CIED	1	64M	70.0	HCC	(*39*)

Abbreviation: M, male; F, female; ICG-R15, ICG plasma retention in 15 minutes; HCC, hepatocellular carcinoma; CRLM, colorectal carcinoma liver metastasis.

shaped red blood cells (*23,42*). With the exception of observation of basic features, this study focused on the hereditary characteristics of CIED. The pedigree investigation showed that the patient was born to parents with consanguineous marriage. Including the reported case, 9 of 12 living family members received ICG testing, of which 6 showed markedly elevated ICG-R15 (> 78%), and 1 had a moderately elevated value (31.5%). The familial clustering is consistent with CIED being a congenital disorder and supports an autosomal recessive mode of inheritance. Notably, no direct evidence was observed to suggest that CIED corelates with hereditary elliptocytosis (*23*). Additionally, extremely high ICG retention rate was also observed in patients with congenital hyperbilirubinemia disorders, including Rotor's syndrome (RS) (*43*), Dubin-Johnson's syndrome (D-JS) (*31*) and Gilbert's syndrome (GS) (*13,21*). However, the genetic interaction among these disorders needs further investigation.

As a brief conclusion, existing evidence suggests that the main feature of CIED is remarkably increased ICG-R15, which is higher than 50% and mostly over 70%. The value of KICG significantly decreases. The ICG plasma disappearance curve demonstrates two distinctive delayed stages: the initial delay and transitional delay in 15-25 minutes after intravenous injection. The binding pattern of ICG to plasma proteins is normal. The laboratory tests of liver functions are within normal ranges or only mildly abnormal, including routine blood and liver biochemistry tests. Additionally, there is no evidence of significant liver impairment consistent with elevated ICG-R15 in histological dimension.

3. Treatment and prognosis for CIED patients with other liver diseases

Most studies noted that this disorder would not be detected unless the patient receives an ICG test. No particular symptoms or pathophysiological changes are observed before and CIED was considered a harmless excretory disorder. Therefore, except for the treatment of primary diseases, previous reports did not provide CIED patients with particular interventions (*12,13,21,25,26*).

In the early years, CIED patients were identified because they occasionally received ICG tests. After the Makuuchi's criteria were established and widely adopted, ICG test was widely applied as a credible preoperative HFR assessment (*11,44*). More CIED cases emerged in the liver surgery area. To date, as detailed in Table 1, 9 CIED cases receiving hepatectomy were reported, in which 6 were HCC patients, 2 were biliary cystadenocarcinoma, and 1 was cavernous hemangioma. The first CIED case receiving hepatectomy was reported by Gotoh *et al*. (*24*). The preoperative examinations of ultrasonography (US), computerized tomography (CT) and percutaneous cystography revealed a cystic lesion located at the left lobe and a connection between gallbladder and liver. Other laboratory tests were unremarkable. But ICG testing showed a significant retention, in which ICG-R15 was 99.8%. The findings supported the diagnosis of biliary cystadenocarcinoma and CIED. The left lobectomy was subsequently conducted successfully. The histology examination showed cystadenocarcinoma cells and normal liver background, consistent with preoperative diagnosis. This research first pointed out that CIED is not a contraindication to hepatectomy (*24*). However, this operation was empirically performed, without other preoperative assessments of HFR, which is dangerous for patients with unexplained high ICG retention.

The other 8 cases reported similar findings (Table 1). Except for one case with D-JS and conjugated hyperbilirubinemia (*31*), other potential causes of high ICG plasma retention, such as severe cirrhosis, intrahepatic vascular shunts, or hyperbilirubinemia were excluded in the remaining cases that underwent surgical treatment (*24,27,28,30,32,34,39,40*). The available levels of tumor markers including alpha-fetoprotein, protein induced by vitamin K absence or antagonist-II, carcinoembryonic antigen, and carbohydrate antigen 19-9 were within normal ranges or moderately increased. Repeated preoperative ICG tests all demonstrated similar significant delay. Various alternative preoperative assessments were implied. Seven of these cases employed ^{99m}Tc-galactosyl human serum albumin liver scintigraphy (^{99m}Tc-GSA) as a supplementary assessment for HFR (*27-29,31,32,34,39*). One of them implied enhanced CT and magnetic resonance imaging (MRI) as supplementary assessments (*30*) and one case implied liver biopsy preoperatively (*28*). None of the methods detected signs of severe liver impairment correlating with the markedly elevated ICG-R15 values. Among these methods, ^{99m}Tc-GSA liver scintigraphy was recognized as the most valuable for assessing unexplained high ICG-R15 (*27-29,31,32, 34,35,39*). The radioactive concentration distribution and quantitative parameters could provide viable evaluations of HFR (*35*).

It is worth noting that only one recent case by Morikawa *et al.* was performed using laparoscopy. The preoperative situation was similar to previous cases, indicating CIED. With normal liver function and ^{99m}Tc-GSA liver scintigraphy results, the patient successfully underwent laparoscopic anatomical liver resection. This study suggested intraoperative ICG fluorescence guidance remains feasible in CIED and proposed that negative staining with 2.5 mg intravenous ICG injection during the operation provides optimal surgical guidance (*39*).

Notably, gadolinium ethoxybenzyl diethylenetriaminepentaacetic acid is a common paramagnetic magnetic resonance contrast agent, which is specifically absorbed by hepatocytes and excreted through biliary and partially urinary systems (*45*). The gadoxetic acid-enhanced MRI (EOB-MRI) is a widely applied examination of hepatobiliary lesions with excellent sensitivity (*46,47*). However, a study by Masuoka *et al.* observed that EOB-MRI presented decreased parenchymal signal intensity and impaired lesion detectability in CIED patients (*37*). It was believed the underlying cause was that gadoxetic acid shares the same hepatic uptake pathway with ICG. The low expression of related transporters in CIED decreases the liver uptake of gadoxetic acid (*16,37,38*).

All hepatic resections were completed successfully, with patients experiencing uncomplicated recoveries (*24,27,28,30-32,34,39,40*). However, postoperative ICG tests indicated that ICG excretion remained markedly delayed (*27,29,31,39*). The long-term observation showed that it would take at least 1 month to completely eliminate ICG in CIED patients (*39*). Additionally, no evidence suggested that CIED either accelerates or moderates the progression of liver tumor or other diseases.

4. The pathogenesis of CIED

Following intravenous injection, ICG generally circulates as follows: (*i*) binding to plasma proteins, mainly albumin and lipoproteins, (*ii*) hepatic delivery *via* blood flow, (*iii*) uptake by hepatocytes as organic anions, (*iv*) direct biliary excretion without metabolism or enterohepatic circulation. Previous studies have affirmed in CIED, that the ICG binding pattern with plasma protein and excretion to biliary tract is the same as in normal people (*12,13*). Therefore, the reason of CIED is possibly localized to the dysfunction of hepatic uptake.

In the past decades, the exploration of hepatocytes' transportation systems has been broadly conducted and gained plenty of advancements (Figure 2) (*48-51*). The channels for organic anion transport in hepatocytes have been identified as Na^+-independent organic anion transporters and Na^+-taurocholate cotransporting polypeptides (NTCPs). The Na^+-independent organic anion transporters can be further classified into organic anion transporters (OATs) and organic anion transporting polypeptides (OATPs) (*15,52-54*). Among these, OATP1B1, OATP1B3 and OATP2B1 isoforms are specifically expressed on the basolateral membrane of human hepatocytes. These OATPs have been demonstrated to mediate the transport of various organic anions, including bilirubin, bile acids and drugs (*55*). Moreover, the observed inhibitory effect of ICG on the transport of the aforementioned substrates suggests that ICG might utilize the same transportation pathways

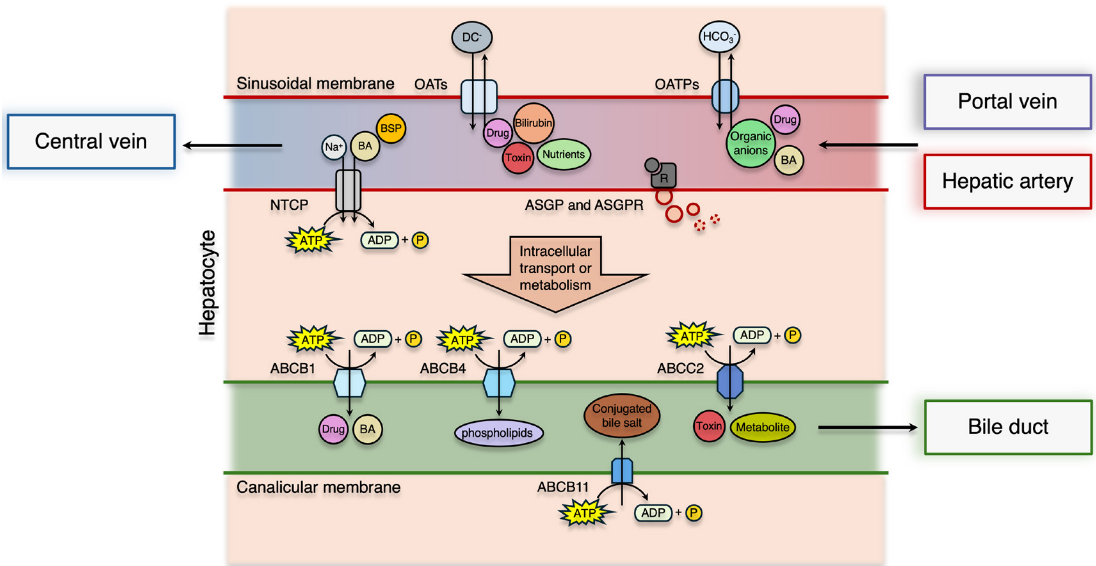

Figure 2. A scheme for the human hepatocyte transport systems. Regarding the transporters located on the sinusoidal membrane, sodium taurocholate co-transporting polypeptide (NTCP) is a unidirectional, ATP and sodium ion dependent transporter, which uptakes conjugated bile acids (BAs), partially unconjugated BAs, bromosulphophthalein (BSP), and thyroid hormones (*50*). Organic anion transporters (OATs) are bidirectional, ATP-independent transporters, including OAT2, OAT3, OAT5, and OAT7. OATs mediate the uptake of common drugs (such as nonsteroidal anti-inflammatory drugs, antibiotics, diuretics), toxins (such as mercury, aristolochic acid), nutrients (such as vitamins, flavonoids), and bilirubin. OATs are driven by the exchange of dicarboxylates (DC^-). Organic anion transporting polypeptides (OATPs) are also bidirectional, ATP-independent transporters, including OATP1B1, OATP1B3, and OATP2B1, which mediate the uptake of drugs, endogenous and exogenous organic anions, and partial BAs. OATPs are driven by the export of bicarbonate (HCO_3^-) (*51*). Asialoglycoprotein (ASGP) specifically binds with the asialoglycoprotein receptor (ASGPR) and forms complex, mediating the subsequent endocytosis. As for the transporters located on the bile canalicular membrane of hepatocytes, most belong to ATP-binding cassette (ABC) family, which are ATP-dependent unidirectional export transporters. ABCB1, formally called multi-drug resistance protein 1 (MDR1) or permeabilization glycoprotein, mediates the export of hydrophobic drugs, anticancer agents, and some bile acids. ABCB4, formally called multi-drug resistance protein 2 (MDR2), mediates the export of phospholipids, particularly phosphatidylcholine, into bile for bile formation, which helps the secretion of bile salts and lipids into the bile canaliculus. ABCB11, formally called bile salt export pump (BSEP), mediates the export of conjugated bile salts. ABCC2, formally called multidrug resistance-associated protein 2 (MRP2), mediates the export of metabolite and toxin (*49*).

(*19*). Subsequently, de Graaf *et al*. affirmed by cellular experiments that OATP1B3 and NTCP are the main transporter of ICG (*16*). Another study by Vaz *et al.* pointed out that defective NTCP expression is typically accompanied by conjugated hypercholanemia, which features extremely high concentrations of conjugated bile salts with relatively mild symptoms (*56*).

With these essential conclusions, further investigation about the expression of OATP1B3 and NTCP in CIED patients was conducted by Kagawa *et al.* In their study, no NTCP-associated hypercholanemia was observed, ruling out the deficiency of NTCP expression as the underlying cause. Therefore, they suggested the absence of OATP1B3 expression was the ultimate reason of CIED. As a result, the hepatic uptake of ICG is accomplished by passive diffusion, significantly limiting the transport efficiency. At the genetic level, the study revealed the deficiency was caused by a homozygous mutation of L1 retrotransposon insertion in *Solute Carrier Organic Anion Transporter Family Member 1B3* (*SLCO1B3)*, which encodes OATP1B3 (*33*). Another follow-up study by Anzai *et al.* observed that heterozygous *SLCO1B3* null mutations did not affect OATP1B3 expression levels, remaining comparable to those in wild-type individuals. Additionally, they confirmed that heterozygous *SLCO1B3* alteration does not result in CIED (*36*), supporting an autosomal recessive inheritance pattern for this condition.

Recently, a retrospective study by Tanimoto *et al.* validated the conclusions with a larger cohort. Among 49 patients who underwent hepatectomy and preoperative ICG tests, absence of OATP1B3 expression was observed in 6 patients, all of whom exhibited characteristic CIED features. Genetic analysis of available frozen tissue blocks confirmed homozygous *SLCO1B3* alterations in all 6 cases. Furthermore, in a separate cohort of 59 colorectal liver metastasis (CRLM) patients, heterozygous alterations of *SLCO1B3* were detected in 5 patients. It's worth noting that these heterozygous carriers showed no significant differences in ICG test results compared to wild-type *SLCO1B3* patients, which is consistent with previous findings (*38*).

Previous studies mentioned that extremely high ICG retention rate was also observed in patients with congenital hyperbilirubinemia disorders, including RS (*43*), D-JS (*31*) and GS (*13,21*). A study by van de Steeg *et al.* affirmed that in RS patients, complete OATP1B1 and 1B3 deficiency leads to the Rotor-type hyperbilirubinemia and ICG excretory defect (*57*). Nambu and Namihisa reported that the average values of ICG-R15 and KICG of 21 D-JS patients were 10.4% and 0.167 respectively, compared to the average values of 73% and 0.020 in 20 CIED patients. Thereby, they indicated that the ICG values are within normal ranges in D-JS (*26*), with reported cases of concurrent CIED and D-JS representing coincidental occurrences (*31*). Many studies have confirmed that hyperbilirubinemia in GS is caused by decreased activity of bilirubin-UDP glucuronosyl transferase (*58*). However, a previous study pointed out that a defect of hepatic organic anion transport could not be attributed to such deficiencies (*59*).

Figure 3 illustrates the difference in ICG circulation

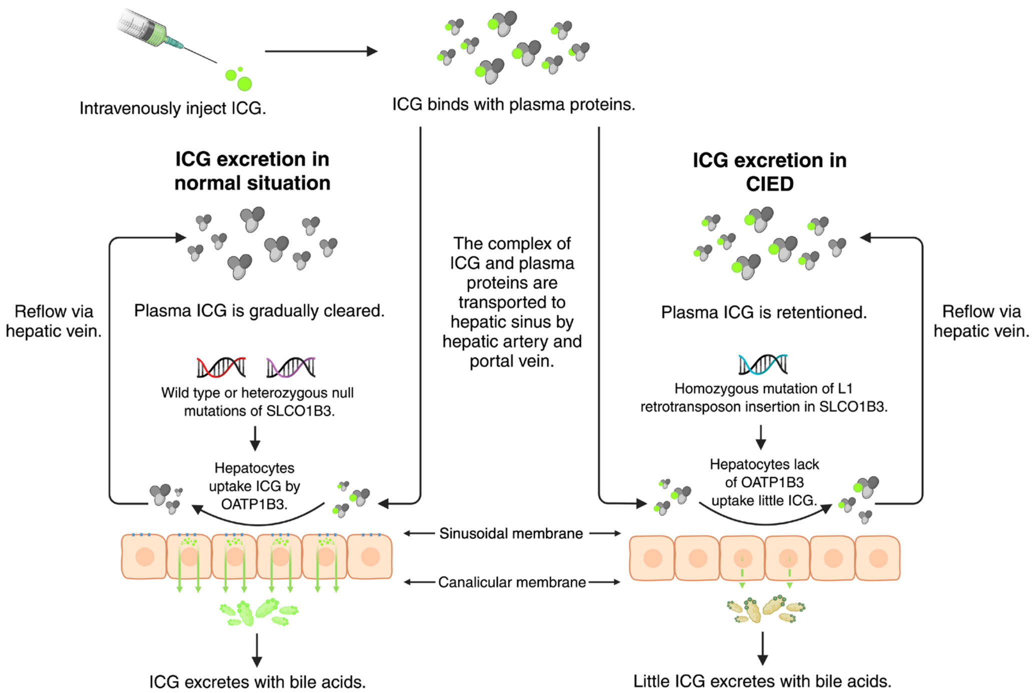

Figure 3. A comparison of ICG excretion patterns in normal circumstances versus in CIED cases. ICG: indocyanine green, OATP1B3: organic anion transporting polypeptide 1B3.

Table 2. Specific subtracts of OATP1B3

Category	Examples	*Ref.*
Exogenous compounds		
Drugs		
Lipid-lowering drugs	rosuvastatin, pitavastatin	(*65*)
Antihypertensive drugs	valsartan, telmisartan, olmesartan, enalapril	
Antidiabetic drugs	repaglinide	
Antibiotics	rifampin	
Chemotherapy agents	hydroxyurea, methotrexate, carboplatin, cisplatin, oxaliplatin, docetaxel, paclitaxel, imatinib	
Imaging Agents		
Organic dyes	bromosulphophthalein, indocyanine green	(*51*)
Radioactive scintigraphy agents	^{99m}Tc-mebrofenin, ^{99m}Tc-diethylenetriaminepentaacetic acid–chenodeoxycholic acid conjugate (^{99m}Tc-DTPA-CDCA)	
MRI contrast agents	gadolinium-ethoxybenzyl-diethylenetriaminepentaacetic acid (Gd-EOB-DTPA)	
Toxins	okadaic acid, ochratoxin A	(*64, 66*)
Endogenous compounds		
Bile acids	taurodeoxycholate, cholate, taurocholate, taurochenodeoxycholate	(*62*)
Bilirubin and conjugates	bilirubin, bilirubinmonoglucuronide	
Steroid and steroid metabolites	dehydroepiandrostenone sulfate, estradiol-17β-glucuronide, estrone-3-sulfate	
Gastrointestinal hormones and leukotrienes	cholecystokinin octapeptide 8, leukotriene C4, prostaglandine E2	
Hormones	triiodothyronine, thyroxine	
Toxins	kynurenic acid, indoxyl sulfate,	(*63*)

between normal situations and CIED. Although existing studies have confirmed that OATP1B3 deficiency impairs hepatocellular ICG uptake and sporadic reports have linked CIED to *SLCO1B3* gene mutations, several critical knowledge gaps remain. First, robust evidence from large-scale population studies and *in vivo* experiments is still lacking to definitively establish pathogenicity. Second, the mechanisms underlying elevated ICG plasma retention in certain congenital hyperbilirubinemia disorders remain poorly understood. Importantly, given OATPs' essential role in hepatic drug or metabolite uptake, its deficiency may predispose patients to dose-induced toxicity, though this requires further clinical validation (*33,51,60,61*). Patients suspected of having CIED should exercise extreme caution when exposed to known OATP1B3-specific substrates and structurally similar potential substrates (Table 2) (*62-66*). Monitoring of circulating concentrations and early prevention of dose-related adverse reactions are necessary. Additionally, while early observations of familial clustering suggested CIED may be a congenital disorder (*23*), subsequent studies have failed to systematically investigate its inheritance pattern at the molecular genetic level. These unresolved issues, including population-level prevalence, precise molecular mechanisms, pharmacological implications, and genetic determinants, represent crucial areas for future research to advance our understanding and clinical management of CIED.

5. Reliable identification and alternative HFR assessment in CIED patients

Many factors have been shown to cause the high ICG plasma retention in patients without CIED. The most common reasons are severe fibrosis and cirrhosis, leading to changes of liver hemodynamics and biliary excretion (*15,17,67*). Vascular abnormalities like intrahepatic vascular shunts and portal/hepatic vein thrombosis similarly compromise liver perfusion and contribute to ICG retention (*18*). Additionally, in severe functional insufficiency and hepatitis, liver ICG uptake capacity decreases remarkably (*5,16,20*). Under such circumstances, elevated ICG values typically contraindicate surgical treatment due to the associated hepatic functional impairment. Importantly, unlike these pathological conditions, CIED does not affect the effectiveness and safety of patients undergoing liver operation. This distinction underscores the critical need for accurate preoperative differentiation between CIED-mediated and pathology-driven ICG retention. Current diagnostic challenges highlight two key requirements: (*i*) reliable methods to distinguish CIED from other causes of ICG retention, and (*ii*) validated alternative approaches for HFR assessment when ICG testing is confounded. Although liver biopsy is regarded as a golden criterion in the diagnosis of liver impairments, its invasive nature and occasional technical limitations necessitate alternative diagnostic strategies (*28*). Here we systematically evaluate several clinical examinations for distinguishing CIED from the other causes and providing accurate supplementary HFR assessments.

5.1. Radioactive tracing technology

As previously presented, the application of radioactive tracers in HFR assessment in patients with normal or defective ICG excretion has been widely recognized and sophisticated (*28,29,31,32,34,39,68*). ^{99m}Tc-GSA liver scintigraphy is one of the most prominent methods. The liver elimination of glycoprotein is based on the combination of asialoglycoprotein (ASGP) and asialoglycoprotein receptor (ASGPR) on the cell membrane of hepatocytes (*69*). ^{99m}Tc-GSA is a radiolabeled molecular probe synthesized from GSA, an ASGP analogue, and the radioactive isotope technetium-99m. After intravenous injection, the probes would specifically bind to ASGPRs, which only occurs in hepatocytes. Both the disappearance in blood and the uptake in liver can be measured clearly and continuously (*70*). When hepatocytes are impaired or lesions appear, the number of functional hepatocytes decrease, manifesting as reduced uptake and concentration of ^{99m}Tc-GSA. The general and regional liver function could be demonstrated visually and noninvasively by single photon emission computed tomography (SPECT). The quantitative indexes could also be calculated, of which the mostly used are LHL15 (receptor index), HH15 (blood clearance index) and GSA-Rmax (regional maximal removal rate) (*18,71-74*). A recent study revealed HH15 and LHL15 have good capacity in predicting ICG-R15 $\geq$ 20%, with AUC of 0.844 (95%CI: 0.747–0.915) and 0.878 (95%CI: 0.759–0.944) respectively (*75*). Thereafter, the development of dynamic SPECT/CT fusion imaging technology sparked new ideas for preoperative liver function assessment. Using the new method, Mao *et al.* proposed a prediction system of the uptake index (UI) and three-dimensional (3D) reconfigurations including overall and future liver remnant (FLR) functions. The UI value was calculated from the dynamic radioactive intensity caused by hepatic uptake and degradation processes of ^{99m}Tc-GSA, quantifying the risk of developing PHLF. Concomitantly, the 3D reconfigurations provide visualized and intuitive information for surgeons to evaluate surgical plans and risks (*76*).

Additionally, Okabayashi *et al.* proposed a prediction index for postoperative remnant liver function, the remKGSA, which is calculated from LHL15 and volumetric rate of the FLR using ^{99m}Tc-GSA SPECT/CT fusion imaging. The index was very useful in predicting safe and accurate liver resection. The researchers pointed out that the remKGSA provides detailed and accurate information to decide whether patients would benefit from surgery (*70*). Furthermore, another study by Sumiyoshi *et al.* affirmed the efficiency of remKGSA in 13 patients with abnormally deteriorated ICG values. It presented that only 3 patients receive hepatectomy along with the Makuuchi's criteria. While the other 10 patients received operations exceeding the criteria and no postoperative mortality occurred in all patients. The study supported the conclusion that the technology would provide accurate assessments of liver function in patients with severely deteriorated ICG levels (*35*). Generally, SPECT/CT fusion technology not only overcomes CT's deficit of estimating liver volume without assessing liver function but also eliminates SPECT's disadvantage of low spatial resolution. Evidence to date suggests it is a reliable assessment technique for liver surgery, including surgery for CIED patients. However, the widespread adoption of this technology is limited by its high costs and technical complexities to some extent, demanding further improvement.

Notably, in addition to ^{99m}Tc-GSA, ^{99m}Tc-mebrofenin hepatobiliary scintigraphy (HBS) is another common radioactive tracing technology for HFR assessments (*77*). However, studies have indicated that the ^{99m}Tc-mebrofenin shares a similar pharmacokinetic pathway with ICG; both undergo hepatic uptake mediated by OATP1B1 and OATP1B3 (*16,78*). Given this mechanistic overlap, the applicability of ^{99m}Tc-mebrofenin HBS in CIED patients remains uncertain, as no studies have yet investigated its performance in this specific population. Therefore, although the ^{99m}Tc-mebrofenin HBS has demonstrated excellent capacity and reliability in liver surgery, it demands more relevant research to explore its application in CIED (*77,79,80*).

5.2. Serum examination and clinical score systems

Plasma bilirubin levels provide basic information about the metabolism and excretion function of the liver. Increasing bilirubin levels act as specific markers for the impairment and loss of function of the liver (*6*). Besides, albumin and proteins related to hemostasis and fibrinolysis are used as indirect indicators of liver synthesis functions (*5*). Based on such biochemistry parameters and common symptoms of insufficient liver function, clinical grading systems like the Child-Pugh score were developed and gained broad application on a global scale (*4*). According to present experience, Child-Pugh scores could provide valuable information in selection of patients with liver diseases for resection or transplantation (*2,3*). Previous case reports also mentioned the application of Child-Pugh scores in CIED patients, which affirmed its effectiveness in assessing surgical tolerance (*39,40*). However, relatively strong subjectivity and poor differentiation capacity weaken the accuracy of the Child-Pugh score. Thorough discussions of its limitations have been conducted (*2,3*). In addition, another common clinical score system, the model for end-stage liver disease (MELD), faces similar troubles, which is narrow for patients undergoing a hepatectomy (*5*).

Based on Child-Pugh scores, Johnson *et al*. proposed an objective score system, albumin-bilirubin score (ALBI), literally calculated by the 2 laboratory values. This international multicenter clinical research provides solid evidence that it has better distinctiveness than conventional Child-Pugh scores in HCC patients' HFR assessment and prognosis prediction. In particular, a significant discrepancy in median survival was observed among patients classified as Child-Pugh A, and subdivided into ALBI grade 1 and 2, which is over 10 months in different country cohorts. ALBI, thereby, provides further information for surgeons to decide treatment plans (*81*). So far, the ALBI score has gained worldwide recognition and has become a crucial component of the preoperative assessment for hepatic surgery (*82-84*).

Subsequently, considerable efforts were dedicated to enhancing the discriminatory and predictive capabilities of the ALBI score. A. Hiraoka *et al*. advised that in addition to the liver function state, the disease burden would also affect the treatment strategies and prognosis of patients, which could be measured by Tumor Node Metastasis (TNM) staging system. As detailed in Table 3, researchers developed the ALBI-Tumor score (ALBI-T) by combining the ALBI and TNM staging system from the Liver Cancer Study Group of Japan (5^{th} edition) (*85*). The results revealed that it is a comprehensive clinical score for strategic decisions and predicting survival of HCC patients (*82,86*). The research team also made efforts to promote the differentiation ability of ALBI scores. The new cut-off value was derived from the ALBI value with the ICG-R15 < 30%, which is believed to be the limit of the minimal anatomical resection in Makuuchi's criteria (*11,87*). As for the results, a good correlation between ALBI and ICG-R15 was observed (r = 0.563; 95%CI: 0.550–0.570; p < 0.0001). The new cut-off value of the modified-ALBI score (mALBI) was -2.27, with an AUC of 0.828 (95%CI: 0.823–0.833). The subsequent studies were conducted in different centers around the world, further affirming its value in clinical practice (*88,89*). Besides, the utility of mALBI in CIED patients was validated, thereby indicating the mALBI as a reliable and effective method for the detection and evaluation of such patients (*38*).

Other studies attempted to reduce the calculation complexity of ALBI scores. Kariyama *et al*. proposed a simplified calculation, the EZ-ALBI, avoiding the logarithmic change of serum total bilirubin. The validation of the effectiveness of EZ-ALBI and EZ-ALBI-T showed that they performed excellently like the previous scores, with a correlation coefficient of 0.981 (95%CI: 0.980-0.982). The researchers highlighted that the simplicity of EZ-ALBI allows clinical workers to mentally perform the calculation and grasp HFR intuitively (*90*).

Moreover, a variety of dimensions of HFR assessment were integrated into the ALBI to enhance its comprehensiveness. Some researchers advised that the platelet counts should be integrated into the ALBI scores, as it is an effective surrogate metric for evaluating portal hypertension (PHT). Liu *et al*. incorporated blood platelet counts into ALBI, thereby forming the PALBI (Table 3). The following studies further corroborated the utility of PALBI in HFR assessment and PHLF prediction, demonstrating its equivalence to other ALBI scores (*91-94*). However, the complexity of its calculation limits the application of PALBI to some extent. More efforts were needed to promote its practicability. The ALBI score can also be combined with imaging examinations. Preoperative 3D-CT reconstruction is used as an effective approach to measure FLR volume (*95*). Zou *et al*. proposed that ALBI could compensate for the weaknesses of FLR measurements, which has difficulty in simultaneously assessing the functional state of preserved livers. The results suggested the combination of ALBI and standardized FLR was effective and precise in predicting PHLF (*96*). Similarly to previously mentioned dynamic SPECT/CT fusion imaging, the application of ALBI and FLR in CIED patients is quite promising. To provide adequate evidence, however, more in-depth studies are demanded.

Besides the methods based on ALBI scores, there were other laboratory indexes that could assist in the evaluation of liver function status and HFR. Aspartate transaminase-Platelet-ratio-index (APRI), first proposed by Wai *et al.* , was originally designed for the noninvasive examination of liver fibrosis and cirrhosis (Table 3) (*97*). Further studies highlighted the fact that APRI has an excellent capacity to predict PHLF and postoperative mortality, due to the reason that such risks are highly related to liver fibrosis or cirrhosis (*98,99*). Recent studies focused on the combination of the ALBI scores and APRI. The results indicated that simultaneous consideration of HFR and severity of liver cirrhosis promotes the accuracy of preoperative assessment and safety of surgery (*100,101*). The four-factor fibrosis index (FIB-4) is another non-invasive tool for the examination of liver cirrhosis (Table 3) (*102*). Recent studies also highlighted the capacity of FIB-4 as an independent predictor of prognosis and post-operative outcomes (*103,104*). H. Toyoda and P. J. Johnson comprehensively discussed the fluctuation trends of the above scores at different stages of liver disease progression. The ALBI scores increase before cirrhosis develops, providing sensitive detection of early liver function deterioration. They are also closely associated with cirrhosis indicators, FIB-4 and APRI, in the progression of liver disease. In the late stages of liver disease, ALBI scores have a comparable ability to MELD and Child-Pugh scores to predict mortality (*84*).

5.3. Imaging examination

Common preoperative imaging examination includes CT, US and MRI. These imaging diagnostic technologies provide comprehensive diagnostic information, offering both direct visualization of liver anatomy and pathological lesions (including location, size and characteristics) and functional estimation of HFR (*105*). First, it is widely accepted that preoperative CT is one of the indispensable preparations for the evaluation of FLR, liver anatomy, cirrhosis and PHT, which are all essential references for treatment decisions (*95,106-108*). Previous case reports pointed out that in CIED

Table 3. A summary of assessments based on serum biomarkers

Author	Time	Name	Formula	Cut-off value	Advantages	*Ref.*
Johnson, *et al.*	2015	ALBI	$ALBI=[ALB\times(-0.085)]+(\log_{10}STB\times0.66)$ *ALB*(*g/L*), *STB*(*μmol/L*)	ALBI-1:(-∞,-2.66] ALBI-2:(-2.66,-1.39] ALBI-3:(-1.39,+∞)	Objective, accurate score for FLR assessment	(*81*)
Liu, *et al.*	2017	PALBI	$PALBI=(2.02\times\log_{10}STB)+[-0.37\times(\log_{10}STB)^2]+(-0.04\times ALB)+(-3.48\times\log_{10}PLT)+[1.01\times(\log_{10}PLT)^2]$ *ALB*(*g/L*), *STB*(*μmol/L*), *PLT*(10^3/*μL*)	PALBI-1:(-∞,-2.53] PALBI-2:(-2.53,-2.09] PALBI-3:(-2.09,+∞)	Objective, accurate score for FLR assessment including portal hypertension	(*91*)
Hiraoka, *et al.*	2016	ALBI-T	***ALBI-T=ALBI Grade+TNM-2*** *ALB*(*g/L*), *STB*(*μmol/L*),*TNM*(*LCSGJ 5th edtion*)	Grade 0~5	Objective, accurate, and comprehensive score including FLR and disease burden	(*86*)
Hiraoka, *et al.*	2017	mALBI	$ALBI=[ALB\times(-0.085)]+(\log_{10}STB\times0.66)$ *ALB*(*g/L*), *STB*(*μmol/L*)	mALBI-1:(-∞,-2.66] mALBI-2a:(-2.66,-2.27] mALBI-2b:(-2.27,-1.39] mALBI-3:(-1.39,+∞)	More delicate stratifications	(*87*)
Kariyama, *et al.*	2020	EZ-ALBI	***EZ-ALBI=STB-9ALB*** conversion with ALBI: [*ALBI*]=0.099[*EZ-ALBI*]+0.81; [*EZ-ALBI*]=9.75[*ALBI*]-9.1 *STB*(*mg/dL*), *ALB*(*g/dL*)	EZ-ALBI-1:(-∞,-34.4] EZ-ALBI-2:(-34.4,-22.2] EZ-ALBI-3:(-22.2,+∞)	Simplified calculation, with the same objectivity and accuracy	(*90*)
Wai	2003	APRI	$APRI=\frac{AST\times100}{PLT}$ *AST*(*/UNL*), *PLT*(10^9/*L*)	A: (0,0.5] B: (1.5, +∞) q1C: (0,1.0] D: (2.0, +∞)	Simple, noninvasive examination of liver fibrosis and liver cirrhosis	(*97*)
Vallet-Pichard	2007	FIB-4	$FIB-4=\frac{Age\times AST}{PLT\times\sqrt{ALT}}$ *Age*(*years*),*AST*,*ALT*(*U/L*), *PLT*(10^9/*L*)	FIB-4A: (0,1.45] FIB-4B: [1.45,3.25] FIB-4C: (3.25,+∞)	Simple, noninvasive examination of liver fibrosis and liver cirrhosis	(*102*)

Abbreviation: ALB, albumin; STB, serum total bilirubin; PLT, platelet; AST, aspartate transaminase; ALT, alanine transaminase.

patients, enhanced CT remains an effective method for evaluating liver volume and structure (*28,30-32,34,39*). Beyond anatomical assessment, CT-based parameters are also promising as alternative HFR assessments. The combination of CT with other HFR assessments, such as ALBI scores, could promote its utility (*96*). In addition, Tu *et al*. proposed a novel CT-based approach to assess HFR, which incorporates both quantitative and qualitative parameters of FLR. It included an index and a grading system, the percentage of remnant liver volume (PRLV) and CT grade, for the assessment of HFR (Table 4). The results revealed that the two parameters correlate with postoperative survival. The combination of them formed a brief prediction line for the evaluation of HFR. The line showed that for patients with better liver status (lower CT grade), a larger resection range (lower PRLV) would be acceptable (*109*). Other studies focused on the effectiveness of dividing spleen or liver volume by body surface area (BSA), including SV_{BSA} and LV_{BSA}, both of which are useful in the assessment of cirrhosis, PHT and HFR (*75,110-112*).

Enhanced multiphase CT provides richer information. Iodine-uptake parameters, such as extracellular volume fraction (ECV) and iodine washout rate (IWR), have been proposed as potential indicators of cirrhosis and HFR (Table 4). Initiated by the deposition of collagen and matrix proteins, the enlargement of ECV is another feature of cirrhosis, which could be precisely measured by enhanced CT (*113-115*). IWR reflects the change of intrahepatic hemodynamics. In livers with severe cirrhosis, the parenchymal demonstrates prolonged iodine retention and reduced IWR. The integration of CT images with IWR could visualize the heterogeneous fibrosis deposition spatially, including the tumor area, which is valuable for surgery (*116*). Furthermore, the previously mentioned study by Nagayama *et al*. compared several common methods in HFR assessment, including IWR, ICG-R15, SV_{BSA} and LV_{BSA}, ^{99m}Tc-GSA liver scintigraphy. The results revealed that all the CT measured indicators correlate with ICG-R15. Among them, IWR, SV_{BSA} and LV_{BSA} are independent predictors of severe liver function insufficiency of ICG-R15 ≥ 20%. The IWR performs the best discriminative capacity with an AUC of 0.845 (95%CI: 0.698–0.931). They also pointed that the combined CT model of IWR and volumetric indicators could provide more accurate evaluation, with an AUC of 0.924 (95%CI: 0.860–0.965), compared to SV_{BSA} and LV_{BSA} with AUCs of 0.653 (95%CI: 0.501–0.790) and 0.694 (95%CI: 0.553–0.820) respectively (*75*).

In summary, current evidence supports the use of CT-derived parameters as objective, accurate, and clinically accessible tools for HFR assessment. These imaging indicators provide reproducible quantitative data that can enhance preoperative risk stratification and surgical planning. However, further large-scale validation studies are warranted to strengthen the reliability of these findings and explore their broader applications in HFR

Table 4. CT-based assessments for hepatic functional reserve

Author	Time	Name	Formula	Cut-off value	*Ref.*
Tu, *et al.*	2007	PRLV	***PRLV*=*pRLV*/*pTLV*×100%** ***pTLV***=121.75+16.49×*body mass* ***pRLV***=*pTLV*-(*tumor volume*+*peritumor volume*) *volume*(*ml*),*body mass*(*kg*)	CT Grade-1: SI<300, with no sign of PVH CT Grade-2: 300<SI<600, with 2~3 signs of PVH CT Grade-3: SI>600 with 3~4 PVH signs, moderate ascites(≤2cm) CT Grade-4: SI>600 with 3~4 PVH signs, severe ascites(>2cm)	(*109*)
		CT Grade	***spleen index*=*diameter of thickness*×*diameter fore and aft*×*diameter up and down*** *diameter* (*cm*)		
Nagayama, *et al.*	2025	IWR	***IWR*=(1-*HE*$_{DP}$/*HE*$_{PVP}$)×100**	ICG≥20%: ≤35.9%	(*75*)
		ECV	***ECV*=(*HE*$_{DP}$×(100-*Hct*))/*AE*$_{DP}$**	ICG≥20%: ≥30.2%	
		SV_{BSA} LV_{BSA}	***SV*$_{BSA}$=*SV*/*BSA*** ***LV*$_{BSA}$=*LV*/*BSA*** *volume*(*ml*),*body surface area*(m^2)	ICG≥20%: ≤705.8 mL/m^2 ICG≥20%: >156.8mL/m^2	

Abbreviation: PRLV, percentage of remnant liver volume; pRLV, predicted remnant liver volume; pTLV, predicted total liver volume; SI, spleen index; PHT, portal hypertension; ECV, extracellular volume; HE, hepatic enhancement; AE, aortic enhancement; Hct, hematocrit level; PVP, portal vein phase; DP, 3minutes delayed phase; SV, spleen volume; LV, liver volume; BSA, body surface area.

evaluation. Additionally, the development of integrated automated algorithms incorporating multiparametric CT data with machine learning techniques could significantly improve standardization, reduce interobserver variability, and optimize clinical workflow, thereby facilitating wider adoption in routine practice.

The applications of non-invasive US examination in liver fibrosis and cirrhosis are well developed (*117*). Common US evaluating dimensions include hepatic and splenic morphology, stiffness changes, and hemodynamic alterations (*118*). Transient elastography and shear wave elastography represent two main technologies in organ stiffness measurement, with substantial evidence supporting their accuracy and efficiency in the early diagnosis and evaluation of liver fibrosis (*119-121*). These elastographic methods also demonstrate clinical utility in assessing splenomegaly, a hallmark complication of PHT, thereby providing valuable diagnostic information to evaluate PHT and cirrhosis (*122,123*). Moreover, recent studies revealed that the US-measured stiffness and volume of liver and spleen could provide predictive information of PHLF (*124,125*). Hemodynamic alteration is another key manifestation of PHT and cirrhosis, which demonstrates increased hepatic venous pressure gradient, decreased portal vein velocity, and portal and total hepatic perfusion. Some studies reported that the doppler US was a potential tool to preliminarily evaluate the portal vein velocity to provide the degree of PHT (*126,127*).

Conventional MRI provides superior soft-tissue contrast for morphological information (*118*), while advanced MR techniques provide functional assessment capabilities. The ECV measured by MR T1 mapping technology could also be useful in the identification and assessment of cirrhosis (*128*). MR elastography has emerged as a particularly promising assessment for liver fibrosis, demonstrating superior sensitivity and specificity in identification of hepatic cirrhosis compared to other non-invasive methods (*129,130*). However, EOB-MRI, while providing excellent hepatobiliary lesion characterization in normal liver function (*46*), appears to have limited diagnostic performance in patients with CIED due to impaired hepatic contrast agent uptake (*37,46*) This limitation significantly reduces its clinical utility in such populations despite its otherwise excellent imaging capabilities.

6. Conclusion

CIED represents a rare dye metabolism disorder characterized solely by markedly elevated plasma ICG retention without other distinctive clinical or laboratory findings. While current research has elucidated the fundamental mechanisms underlying CIED, significant knowledge gaps remain regarding its precise pathogenesis in certain congenital hyperbilirubinemia disorders and its inheritance patterns. The published literature on CIED epidemiology, clinical characteristics, management strategies, and prognostic outcomes is limited not only by small sample sizes but also by the inherently low amount of evidence. Given the extreme rarity of CIED, most available data are derived from isolated case reports and small retrospective case series, which are susceptible to selection bias, reporting bias, and incomplete follow-up. To date, there is an absence of large-scale population-based epidemiological investigations and robust prospective cohort studies that could more accurately define incidence, risk factors, and long-term outcomes. Additionally, no convincing *in vivo* experimental models have been established to validate the underlying biological processes, limiting mechanistic interpretation and causal inference. Moreover, another important limitation concerns geographic concentration. Nearly all reported cases originate from Japan and China. The lack of data from other ethnic and geographic populations substantially restricts the assessment of global generalizability. Potential ethnic, genetic, environmental, or practice-related differences cannot currently be evaluated. Future efforts should focus on multinational collaborative investigations and mechanistic studies to clarify epidemiology, validate pathophysiology, and improve risk stratification. Basic research should prioritize the development of reproducible *in vivo* models incorporating susceptibility backgrounds, coupled with intervention and biodistribution studies, to validate causality and define actionable mechanistic targets.

Our review identifies several key modalities for differentiating CIED and supplementing HFR assessment. First, the application and utility of ^{99m}Tc-GSA liver scintigraphy has gained relatively considerable validation. Next, the serum biomarkers and relevant clinical scores like the ALBI scores are quite useful. Finally, most imaging examinations, including CT, US and MR, generally focus on the differentiation and evaluation of cirrhosis and PHT, and provide detailed anatomy information of liver and lesions. Several of them provide assessment of HFR. CT is widely applied due to its affordability and rich information, making it an indispensable examination in CIED. Notably, due to the impaired lesion detectability observed in CIED patients, it is lamentable that the utility of EOB-MRI is rather limited. Based on existing findings, we proposed a strategy to cope with unexplained high ICG retention patients (Figure 4). In our perspective, this strategy would be simple to apply in clinical practice and helpful for such patients. However, it demands further validation. Nowadays, with recent advancement of next-generation screening (NGS), molecular testing technology is playing an increasingly vital role in precise surgery. Genetic testing, whether based on blood or pathological samples, not only provides a detailed molecular diagnosis but also guides perioperative targeted therapy and immunotherapy in different types of malignancy (*131-133*). Although the molecular diagnosis and therapy of HCC remains

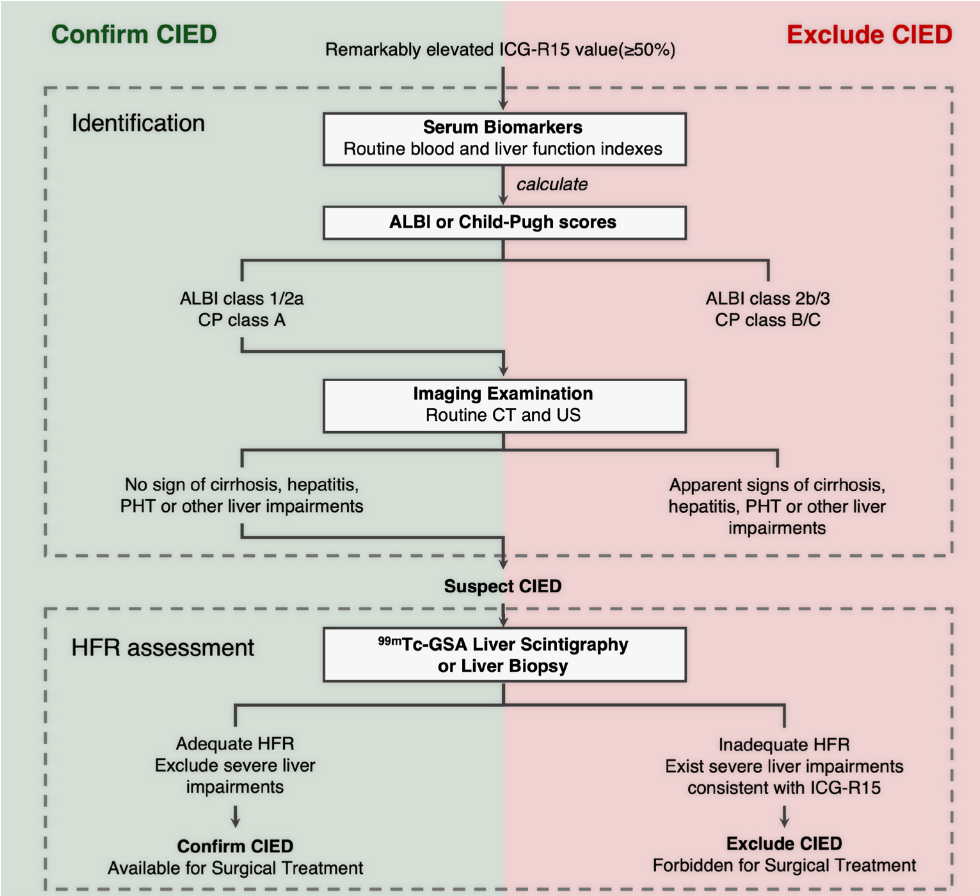

Figure 4. A strategy to cope with unexplained high ICG retention patients. CIED: constitutional indocyanine green excretory defect, ICG-R15: plasma indocyanine green retention rate at 15 minutes, ALBI: albumin-bilirubin scores, CT: computer tomography, US: ultrasonography, PHT: portal hypertension, HFR: hepatic functional reserve, ^{99m}Tc-GSA liver scintigraphy: ^{99m}Tc-Galactosyl human Serum Albumin liver scintigraphy.

divergent, hopefully such high-throughput sequencing technologies could improve *SLCO1B3* mutation screening, thus reducing the cost of CIED diagnosis and assisting with clinical decision-making (*134*).

The expanding use of ICG tests in hepatic surgery will likely increase CIED detection rates, underscoring the importance of reliable diagnostic and assessment protocols. However, the rarity of CIED has constrained study sizes, necessitating external validation of current findings in larger populations. Future research should prioritize multicenter studies to validate existing diagnostic algorithms, develop of standardized assessment protocols, and investigate novel functional imaging parameters. The proposed diagnostic strategy balances clinical practicality with comprehensive evaluation, though its implementation requires further validation. As hepatic surgery advances, establishing evidence-based approaches for CIED management will become increasingly crucial for optimal patient care and surgical outcomes.

Acknowledgements

We would like to appreciate all the staff in our team for their valuable support.

Funding: This work was supported by a grant from the National Key Research and Development Program of China (No. 2023YFB3810004 for Huang J).

Conflict of Interest: The authors have no conflicts of interest to disclose.

References

1. Dong J, Zheng S, Chen X, Dou K, Fan J, Bie P, Geng X, Lv W. Consensus on evaluation of hepatic functional reserve before hepatectomy (2011 edition). Chin J Dig Surg. 2011; 10:20-25.
2. Fan ST. Liver functional reserve estimation: state of the art and relevance for local treatments: the Eastern perspective. J Hepatobiliary Pancreat Sci. 2010; 17:380-384.
3. Durand F, Valla D. Assessment of prognosis of cirrhosis. Semin Liver Dis. 2008; 28:110-122.
4. Garcea G, Ong SL, Maddern GJ. Predicting liver failure following major hepatectomy. Dig Liver Dis. 2009; 41:798-806.
5. Hoekstra LT, de Graaf W, Nibourg GA, Heger M, Bennink RJ, Stieger B, van Gulik TM. Physiological and biochemical basis of clinical liver function tests: a review.

Ann Surg. 2013; 257:27-36.
6. Woreta TA, Alqahtani SA. Evaluation of abnormal liver tests. Med Clin North Am. 2014; 98:1-16.
7. Kaibori M, Matsui K, Shimada M, Kubo S, Hasegawa K. Update on perioperative management of patients undergoing surgery for liver cancer. Ann Gastroenterol Surg. 2022; 6:344-354.
8. Lau H, Man K, Fan ST, Yu WC, Lo CM, Wong J. Evaluation of preoperative hepatic function in patients with hepatocellular carcinoma undergoing hepatectomy. Br J Surg. 1997; 84:1255-1259.
9. Cherrick GR, Stein SW, Leevy CM, Davidson CS. Indocyanine green: observations on its physical properties, plasma decay, and hepatic extraction. J Clin Invest. 1960; 39:592-600.
10. Caesar J, Shaldon S, Chiandussi L, Guevara L, Sherlock S. The use of indocyanine green in the measurement of hepatic blood flow and as a test of hepatic function. Clin Sci. 1961; 21:43-57.
11. Miyagawa S, Makuuchi M, Kawasaki S, Kakazu T. Criteria for safe hepatic resection. Am J Surg. 1995; 169:589-594.
12. Namihisa T, Nambu M, Kobayashi N, Kuroda H. The constitutional indocyanine green excretory defect--report of four cases. Gastroenterol Jpn. 1975; 10:70-76.
13. Okuda K, Ohkubo H, Musha H, Kotoda K, Abe H, Tanikawa K. Marked delay in indocyanine green plasma clearance with a near-normal bromosulphophthalein retention test: a constitutional abnormality? Gut. 1976; 17:588-594.
14. Namihisa T, Nambu M, Kobayashi N, Kuroda H. Nine cases with marked retention of indocyanine green test and normal sulfobromophthalein test without abnormal liver histology: constitutional indocyanine green excretory defect. Hepatogastroenterology. 1981; 28:6-12.
15. Ott P. Hepatic elimination of indocyanine green with special reference to distribution kinetics and the influence of plasma protein binding. Pharmacol Toxicol. 1998; 83 Suppl 2:1-48.
16. de Graaf W, Häusler S, Heger M, van Ginhoven TM, van Cappellen G, Bennink RJ, Kullak-Ublick GA, Hesselmann R, van Gulik TM, Stieger B. Transporters involved in the hepatic uptake of (99m)Tc-mebrofenin and indocyanine green. J Hepatol. 2011; 54:738-745.
17. Huet PM, Du Reau A, Marleau D. Arterial and portal blood supply in cirrhosis: a functional evaluation. Gut. 1979; 20:792-796.
18. Kwon AH, Ha-Kawa SK, Uetsuji S, Inoue T, Matsui Y, Kamiyama Y. Preoperative determination of the surgical procedure for hepatectomy using technetium-99m-galactosyl human serum albumin (99mTc-GSA) liver scintigraphy. Hepatology. 1997; 25:426-429.
19. Cui Y, König J, Leier I, Buchholz U, Keppler D. Hepatic uptake of bilirubin and its conjugates by the human organic anion transporter SLC21A6. J Biol Chem. 2001; 276:9626-9630.
20. Geier A, Wagner M, Dietrich CG, Trauner M. Principles of hepatic organic anion transporter regulation during cholestasis, inflammation and liver regeneration. Biochim Biophys Acta. 2007; 1773:283-308.
21. Adachi Y, Yamamoto T, Onishi S, Tanaka S, Wakisaka G. The discrepancy between plasma clearance tests of indocyanine green (ICG) and sulfobromophthalein (BSP): --report of cases and a study of ICG-binding pattern of serum proteins. Gastroenterol Jpn. 1976; 11:75-87.
22. Takase S, Takada A, Matsuda Y. Studies on the pathogenesis of the constitutional excretory defect of indocyanine green. Gastroenterol Jpn. 1982; 17:301-309.
23. Taketazu F, Sanada I, Ngamatsu N, Mukai R, Suetomo Y, Toyoda N, Takada M, Hida K, Kubota K, Maezawa M. A case of hereditary elliptocytosis associated with constitutional indocyanine green excretory defect. Jpn J Med. 1984; 23:139-143.
24. Gotoh K, Konaga E, Takeuchi H, Mano S, Kohno H. A case of biliary cystadenocarcinoma arising in the liver with a congenital retention of indocyanine green. Acta Med Okayama. 1992; 46:389-393.
25. Ikejima K, Ichikawa S, Kitamura T, Watanabe S, Hirose M, Yokoi Y, Uchida S, Oide H, Suzuki H, Kitami N. Marked retention of indocyanine green and sulfobromophthalein with chronic persistent hepatitis. J Gastroenterol Hepatol. 1993; 8:489-494.
26. Nambu M, Namihisa T. Hepatic transport of serum bilirubin, bromsulfophthalein, and indocyanine green in patients with congenital non-hemolytic hyperbilirubinemia and patients with constitutional indocyanine green excretory defect. J Gastroenterol. 1996; 31:228-236.
27. Hanazaki K, Wakabayashi M, Makiuchi A, Igarashi J, Sodeyama H, Wada S, Amano J. Hepatectomy of cavernous hemangioma with constitutional indocyanine green excretory defect. Hepatogastroenterology. 2000; 47:1719-1721.
28. Yamanaka N, Shimizu S, Chijiiwa K, Nishiyama K, Noshiro H, Yamaguchi K, Tanaka M. Hepatectomy and marked retention of indocyanine green and bromosulfophtalein. Hepatogastroenterology. 2001; 48:1450-1452.
29. Kadono J, Kumemura H, Nishida S, Nakamura N, Gejima K, Nakajo M, Tsuchimochi S, Matsumoto J, Hamada N, Sakata R. 99mTc-DTPA-galactosyl-human-serum-albumin liver scintigraphy for evaluating hepatic functional reserve before hepatectomy in a patient with indocyanine green excretory defect: report of a case. Surg Today. 2006; 36:481-484.
30. Maeda H, Okabayashi T, Kobayashi M, Sugimoto T, Namikawa T, Okamoto K, Araki K. Hepatectomy for hepatocellular carcinoma with indocyanine green excretory defect: a case report. Hepatogastroenterology. 2007; 54:1810-1812.
31. Aoki H, Morihiro T, Arata T, Kanaya N, Takeda S, Ninomiya T, Seita M, Katsuda K, Tanakaya K, Takeuchi H. Hepatectomy in a hepatocellular carcinoma case with Dubin-Johnson syndrome and indocyanine green excretory defect. Clin J Gastroenterol. 2013; 6:69-74.
32. Imada S, Kobayashi T, Kitao A, Matsui O, Hashimoto M, Ide K, Ishiyama K, Arihiro K, Tashiro H, Ohdan H. Central bisectionectomy for hepatocellular carcinoma in a patient with indocyanine green excretory defect associated with reduced expression of the liver transporter. Surg Case Rep. 2016; 2:89.
33. Kagawa T, Adachi Y, Hashimoto N, Mitsui H, Ohashi T, Yoneda M, Hasegawa I, Hirose S, Tsuruya K, Anzai K, Mine T. Loss of organic anion transporting polypeptide 1B3 function causes marked delay in indocyanine green clearance without any clinical symptoms. Hepatology. 2017; 65:1065-1068.
34. Nakatake R, Ishizaki M, Miyasaka C, Matsui K, Kaibori M. Hepatectomy in a case of hepatocellular carcinoma with constitutional indocyanine green excretory defect. Int J Surg Case Rep. 2018; 53:231-234.

35. Sumiyoshi T, Okabayashi T, Negoro Y, Hata Y, Noda Y, Sui K, Iwata J, Matsumoto M. (99m)Tc-GSA SPECT/CT fusion imaging for hepatectomy candidates with extremely deteriorated ICG value. Jpn J Radiol. 2018; 36:537-543.
36. Anzai K, Tsuruya K, Morimachi M, Arase Y, Hirose S, Hirabayashi K, Adachi Y, Kagawa T. The Impact of a Heterozygous SLCO1B3 Null Variant on the Indocyanine Green Retention Test. J Pharm Sci. 2020; 109:3206-3209.
37. Masuoka S, Nasu K, Takahashi H, Kitao A, Sakai M, Ishiguro T, Saida T, Minami M. Impaired lesion detectability on gadoxetic acid-enhanced MR imaging in indocyanine green excretory defect: case series of three patients. Jpn J Radiol. 2020; 38:997-1003.
38. Tanimoto M, Nishioka Y, Inagaki Y, Kokudo T, Ishizawa T, Arita J, Akamatsu N, Kaneko J, Hasegawa K. Genetic alteration of SLCO1B3 defines constitutional indocyanine green excretory defect in patients who underwent hepatectomy. Hepatol Res. 2024.
39. Morikawa T, Wakui Y, Hasegawa Y, Sugisawa N, Kimura S, Hirashima T, Kinouchi M, Iwasashi H. Laparoscopic Anatomical Liver Resection for the Patients With Constitutional Indocyanine Green Excretory Defect: A Case Report. Asian J Endosc Surg. 2025; 18:e13415.
40. Liu W, Chen LJ, Jiang Y, Xu LJ, Qiu X. Hepatocellular carcinoma with indocyanine green excretory defect: a case report and review of the literature. J Int Med Res. 2021; 49:3000605211004025.
41. Ishigami Y, Masuzawa M, Miyoshi E, Kato M, Tamura K, Kanda M, Awazu K, Taniguchi K, Kurita M, Hayashi N. Clinical applications of ICG Finger Monitor in patients with liver disease. J Hepatol. 1993; 19:232-240.
42. Soderquist C, Bagg A. Hereditary elliptocytosis. Blood. 2013; 121:3066.
43. Kawasaki H, Kimura N, Irisa T, Hirayama C. Dye clearance studies in Rotor's syndrome. Am J Gastroenterol. 1979; 71:380-388.
44. Makuuchi M, Kosuge T, Takayama T, Yamazaki S, Kakazu T, Miyagawa S, Kawasaki S. Surgery for small liver cancers. Semin Surg Oncol. 1993; 9:298-304.
45. Tanimoto A, Lee JM, Murakami T, Huppertz A, Kudo M, Grazioli L. Consensus report of the 2nd International Forum for Liver MRI. Eur Radiol. 2009; 19 Suppl 5:S975-989.
46. Huppertz A, Balzer T, Blakeborough A, Breuer J, Giovagnoni A, Heinz-Peer G, Laniado M, Manfredi RM, Mathieu DG, Mueller D, Reimer P, Robinson PJ, Strotzer M, Taupitz M, Vogl TJ. Improved detection of focal liver lesions at MR imaging: multicenter comparison of gadoxetic acid-enhanced MR images with intraoperative findings. Radiology. 2004; 230:266-275.
47. Tsurusaki M, Sofue K, Murakami T. Current evidence for the diagnostic value of gadoxetic acid-enhanced magnetic resonance imaging for liver metastasis. Hepatol Res. 2016; 46:853-861.
48. Nigam SK, Bush KT, Martovetsky G, Ahn SY, Liu HC, Richard E, Bhatnagar V, Wu W. The organic anion transporter (OAT) family: A systems biology perspective. Physiol Rev. 2015; 95:83-123.
49. Kroll T, Prescher M, Smits SHJ, Schmitt L. Structure and Function of Hepatobiliary ATP Binding Cassette Transporters. Chem Rev. 2021; 121:5240-5288.
50. Tan X, Xiang Y, Shi J, Chen L, Yu D. Targeting NTCP for liver disease treatment: A promising strategy. J Pharm Anal. 2024; 14:100979.
51. Hagenbuch B, Stieger B, Locher KP. Organic anion transporting polypeptides: Pharmacology, toxicology, structure, and transport mechanisms. Pharmacol Rev. 2025; 77:100023.
52. Sekine T, Cha SH, Endou H. The multispecific organic anion transporter (OAT) family. Pflugers Arch. 2000; 440:337-350.
53. Hagenbuch B, Meier PJ. Organic anion transporting polypeptides of the OATP/ SLC21 family: phylogenetic classification as OATP/ SLCO superfamily, new nomenclature and molecular/functional properties. Pflugers Arch. 2004; 447:653-665.
54. König J, Seithel A, Gradhand U, Fromm MF. Pharmacogenomics of human OATP transporters. Naunyn Schmiedebergs Arch Pharmacol. 2006; 372:432-443.
55. Ho RH, Tirona RG, Leake BF, Glaeser H, Lee W, Lemke CJ, Wang Y, Kim RB. Drug and bile acid transporters in rosuvastatin hepatic uptake: function, expression, and pharmacogenetics. Gastroenterology. 2006; 130:1793-1806.
56. Vaz FM, Paulusma CC, Huidekoper H, de Ru M, Lim C, Koster J, Ho-Mok K, Bootsma AH, Groen AK, Schaap FG, Oude Elferink RP, Waterham HR, Wanders RJ. Sodium taurocholate cotransporting polypeptide (SLC10A1) deficiency: conjugated hypercholanemia without a clear clinical phenotype. Hepatology. 2015; 61:260-267.
57. van de Steeg E, Stránecký V, Hartmannová H, *et al*. Complete OATP1B1 and OATP1B3 deficiency causes human Rotor syndrome by interrupting conjugated bilirubin reuptake into the liver. J Clin Invest. 2012; 122:519-528.
58. Vítek L, Tiribelli C. Gilbert's syndrome revisited. J Hepatol. 2023; 79:1049-1055.
59. Martin JF, Vierling JM, Wolkoff AW, Scharschmidt BF, Vergalla J, Waggoner JG, Berk PD. Abnormal hepatic transport of indocyanine green in Gilbert's syndrome. Gastroenterology. 1976; 70:385-391.
60. Fahrmayr C, Fromm MF, König J. Hepatic OATP and OCT uptake transporters: their role for drug-drug interactions and pharmacogenetic aspects. Drug Metab Rev. 2010; 42:380-401.
61. Alam K, Crowe A, Wang X, Zhang P, Ding K, Li L, Yue W. Regulation of Organic Anion Transporting Polypeptides (OATP) 1B1- and OATP1B3-Mediated Transport: An Updated Review in the Context of OATP-Mediated Drug-Drug Interactions. Int J Mol Sci. 2018; 19:855.
62. Hagenbuch B, Stieger B. The SLCO (former SLC21) superfamily of transporters. Mol Aspects Med. 2013; 34:396-412.
63. Sato T, Yamaguchi H, Kogawa T, Abe T, Mano N. Organic anion transporting polypeptides 1B1 and 1B3 play an important role in uremic toxin handling and drug-uremic toxin interactions in the liver. J Pharm Pharm Sci. 2014; 17:475-484.
64. Ikema S, Takumi S, Maeda Y, Kurimoto T, Bohda S, Chigwechokha PK, Sugiyama Y, Shiozaki K, Furukawa T, Komatsu M. Okadaic acid is taken-up into the cells mediated by human hepatocytes transporter OATP1B3. Food Chem Toxicol. 2015; 83:229-236.
65. Schulte RR, Ho RH. Organic Anion Transporting Polypeptides: Emerging Roles in Cancer Pharmacology. Mol Pharmacol. 2019; 95:490-506.
66. Wang J, Gan C, Qi X, Lebre MC, Schinkel AH. Human organic anion transporting polypeptide (OATP) 1B3 and mouse OATP1A/1B affect liver accumulation of

Ochratoxin A in mice. Toxicol Appl Pharmacol. 2020; 401:115072.
67. Wissler EH. Identifying a long standing error in single-bolus determination of the hepatic extraction ratio for indocyanine green. Eur J Appl Physiol. 2011; 111:641-646.
68. Kaibori M, Ha-Kawa SK, Maehara M, Ishizaki M, Matsui K, Sawada S, Kwon AH. Usefulness of Tc-99m-GSA scintigraphy for liver surgery. Ann Nucl Med. 2011; 25:593-602.
69. Stockert RJ, Morell AG. Hepatic binding protein: the galactose-specific receptor of mammalian hepatocytes. Hepatology. 1983; 3:750-757.
70. Okabayashi T, Shima Y, Morita S, Shimada Y, Sumiyoshi T, Sui K, Iwata J, Iiyama T. Liver Function Assessment Using Technetium 99m-Galactosyl Single-Photon Emission Computed Tomography/CT Fusion Imaging: A Prospective Trial. J Am Coll Surg. 2017; 225:789-797.
71. Sawamura T, Nakada H, Hazama H, Shiozaki Y, Sameshima Y, Tashiro Y. Hyperasialoglycoproteinemia in patients with chronic liver diseases and/or liver cell carcinoma. Asialoglycoprotein receptor in cirrhosis and liver cell carcinoma. Gastroenterology. 1984; 87:1217-1221.
72. Kondo M. Usefulness of 99mTc-GSA scintigraphy for estimation of residual hepatic functions and postoperative changes of HH15 and LHL15. Kaku Igaku. 2001; 38:191-200.
73. Iimuro Y, Kashiwagi T, Yamanaka J, Hirano T, Saito S, Sugimoto T, Watanabe S, Kuroda N, Okada T, Asano Y, Uyama N, Fujimoto J. Preoperative estimation of asialoglycoprotein receptor expression in the remnant liver from CT/99mTc-GSA SPECT fusion images correlates well with postoperative liver function parameters. J Hepatobiliary Pancreat Sci. 2010; 17:673-681.
74. Kudo M, Todo A, Ikekubo K, Yamamoto K, Vera DR, Stadalnik RC. Quantitative assessment of hepatocellular function through *in vivo* radioreceptor imaging with technetium 99m galactosyl human serum albumin. Hepatology. 1993; 17:814-819.
75. Nagayama Y, Hokamura M, Taguchi N, Yokota Y, Osaki T, Ogasawara K, Shiraishi S, Yoshida R, Harai R, Kidoh M, Oda S, Nakaura T, Hirai T. Liver function estimation using multiphase hepatic CT: diagnostic performance of iodine-uptake and volumetric parameters. Eur Radiol. 2025; 35:5781–5791.
76. Mao Y, Du S, Ba J, *et al*. Using Dynamic 99mTc-GSA SPECT/CT fusion images for hepatectomy planning and postoperative liver failure prediction. Ann Surg Oncol. 2015; 22:1301-1307.
77. Bennink RJ, Dinant S, Erdogan D, Heijnen BH, Straatsburg IH, van Vliet AK, van Gulik TM. Preoperative assessment of postoperative remnant liver function using hepatobiliary scintigraphy. J Nucl Med. 2004; 45:965-971.
78. Trauner M, Meier PJ, Boyer JL. Molecular pathogenesis of cholestasis. N Engl J Med. 1998; 339:1217-1227.
79. Erdogan D, Heijnen BH, Bennink RJ, Kok M, Dinant S, Straatsburg IH, Gouma DJ, van Gulik TM. Preoperative assessment of liver function: A comparison of 99mTc-Mebrofenin scintigraphy with indocyanine green clearance test. Liver Int. 2004; 24:117-123.
80. Bakos A, Libor L, Urbán S, Géczi T, Bukva M, Hőhn J, Lázár G, Nagy A, Farkas I, Sipka G, Pávics L, Besenyi Z. Dynamic [(99m)Tc]Tc-mebrofenin SPECT/CT in preoperative planning of liver resection: a prospective study. Sci Rep. 2024; 14:30305.
81. Johnson PJ, Berhane S, Kagebayashi C, *et al*. Assessment of liver function in patients with hepatocellular carcinoma: a new evidence-based approach-the ALBI grade. J Clin Oncol. 2015; 33:550-558.
82. Hiraoka A, Kumada T, Michitaka K, Kudo M. Newly Proposed ALBI Grade and ALBI-T Score as Tools for Assessment of Hepatic Function and Prognosis in Hepatocellular Carcinoma Patients. Liver Cancer. 2019; 8:312-325.
83. Reig M, Forner A, Rimola J, *et al*. BCLC strategy for prognosis prediction and treatment recommendation: The 2022 update. J Hepatol. 2022; 76:681-693.
84. Toyoda H, Johnson PJ. The ALBI score: From liver function in patients with HCC to a general measure of liver function. JHEP Rep. 2022; 4:100557.
85. Japan Lcsgo. The general rules for the clinical and pathological study of primary liver cancer. The 5th edition. 2009; 24.
86. Hiraoka A, Kumada T, Michitaka K, *et al*. Usefulness of albumin-bilirubin grade for evaluation of prognosis of 2584 Japanese patients with hepatocellular carcinoma. J Gastroenterol Hepatol. 2016; 31:1031-1036.
87. Hiraoka A, Michitaka K, Kumada T, Izumi N, Kadoya M, Kokudo N, Kubo S, Matsuyama Y, Nakashima O, Sakamoto M, Takayama T, Kokudo T, Kashiwabara K, Kudo M. Validation and Potential of Albumin-Bilirubin Grade and Prognostication in a Nationwide Survey of 46,681 Hepatocellular Carcinoma Patients in Japan: The Need for a More Detailed Evaluation of Hepatic Function. Liver Cancer. 2017; 6:325-336.
88. Zhong CR, Qiu JL, Yuan YC, Qiu ZY, Li K, Wang CW, Shi YX, Li KR, Lin Z, Huang ZK, He W, Li BK, Yuan YF. A detailed assessment of liver function in patients with hepatocellular carcinoma *via* the modified albumin-bilirubin (mALBI) grade. Am J Cancer Res. 2022; 12:2711-2720.
89. Hiraoka A, Kumada T, Tsuji K, *et al*. Validation of Modified ALBI Grade for More Detailed Assessment of Hepatic Function in Hepatocellular Carcinoma Patients: A Multicenter Analysis. Liver Cancer. 2019; 8:121-129.
90. Kariyama K, Nouso K, Hiraoka A, *et al*. EZ-ALBI Score for Predicting Hepatocellular Carcinoma Prognosis. Liver Cancer. 2020; 9:734-743.
91. Liu PH, Hsu CY, Hsia CY, Lee YH, Chiou YY, Huang YH, Lee FY, Lin HC, Hou MC, Huo TI. ALBI and PALBI grade predict survival for HCC across treatment modalities and BCLC stages in the MELD Era. J Gastroenterol Hepatol. 2017; 32:879-886.
92. Lu LH, Zhang YF, Mu-Yan C, Kan A, Zhong XP, Mei J, Ling YH, Li SH, Shi M, Wei W, Guo RP. Platelet-albumin-bilirubin grade: Risk stratification of liver failure, prognosis after resection for hepatocellular carcinoma. Dig Liver Dis. 2019; 51:1430-1437.
93. Wang Q, Qiao W, Zhang H, Liu B, Li J, Zang C, Mei T, Zheng J, Zhang Y. Nomogram established on account of Lasso-Cox regression for predicting recurrence in patients with early-stage hepatocellular carcinoma. Front Immunol. 2022; 13:1019638.
94. Wang Q, Sheng S, Xiong Y, Han M, Jin R, Hu C. Machine learning-based model for predicting tumor recurrence after interventional therapy in HBV-related hepatocellular carcinoma patients with low preoperative platelet-albumin-bilirubin score. Front Immunol. 2024; 15:1409443.
95. Simpson AL, Geller DA, Hemming AW, Jarnagin WR,

Clements LW, D'Angelica MI, Dumpuri P, Gönen M, Zendejas I, Miga MI, Stefansic JD. Liver planning software accurately predicts postoperative liver volume and measures early regeneration. J Am Coll Surg. 2014; 219:199-207.
96. Zou H, Wen Y, Yuan K, Miao XY, Xiong L, Liu KJ. Combining albumin-bilirubin score with future liver remnant predicts post-hepatectomy liver failure in HBV-associated HCC patients. Liver Int. 2018; 38:494-502.
97. Wai CT, Greenson JK, Fontana RJ, Kalbfleisch JD, Marrero JA, Conjeevaram HS, Lok AS. A simple noninvasive index can predict both significant fibrosis and cirrhosis in patients with chronic hepatitis C. Hepatology. 2003; 38:518-526.
98. Hung HH, Su CW, Lai CR, Chau GY, Chan CC, Huang YH, Huo TI, Lee PC, Kao WY, Lee SD, Wu JC. Fibrosis and AST to platelet ratio index predict post-operative prognosis for solitary small hepatitis B-related hepatocellular carcinoma. Hepatol Int. 2010; 4:691-699.
99. Shen SL, Fu SJ, Chen B, Kuang M, Li SQ, Hua YP, Liang LJ, Guo P, Hao Y, Peng BG. Preoperative aspartate aminotransferase to platelet ratio is an independent prognostic factor for hepatitis B-induced hepatocellular carcinoma after hepatic resection. Ann Surg Oncol. 2014; 21:3802-3809.
100. Luo H, Li C, Chen L. Preoperative albumin-bilirubin grade combined with aspartate aminotransferase-to-platelet count ratio index predict outcomes of patients with hepatocellular carcinoma within Milan criteria after liver resection. Biosci Trends. 2019; 13:176-181.
101. Starlinger P, Ubl DS, Hackl H, Starlinger J, Nagorney DM, Smoot RL, Habermann EB, Cleary SP. Combined APRI/ALBI score to predict mortality after hepatic resection. BJS Open. 2021; 5:zraa043.
102. Vallet-Pichard A, Mallet V, Nalpas B, Verkarre V, Nalpas A, Dhalluin-Venier V, Fontaine H, Pol S. FIB-4: an inexpensive and accurate marker of fibrosis in HCV infection. Comparison with liver biopsy and fibrotest. Hepatology. 2007; 46:32-36.
103. Toyoda H, Kumada T, Tada T, Kaneoka Y, Maeda A. A laboratory marker, FIB-4 index, as a predictor for long-term outcomes of hepatocellular carcinoma patients after curative hepatic resection. Surgery. 2015; 157:699-707.
104. Zhou P, Chen B, Miao XY, Zhou JJ, Xiong L, Wen Y, Zou H. Comparison of FIB-4 Index and Child-Pugh Score in Predicting the Outcome of Hepatic Resection for Hepatocellular Carcinoma. J Gastrointest Surg. 2020; 24:823-831.
105. Sahani D, Mehta A, Blake M, Prasad S, Harris G, Saini S. Preoperative hepatic vascular evaluation with CT and MR angiography: implications for surgery. Radiographics. 2004; 24:1367-1380.
106. Kubota K, Makuuchi M, Kusaka K, Kobayashi T, Miki K, Hasegawa K, Harihara Y, Takayama T. Measurement of liver volume and hepatic functional reserve as a guide to decision-making in resectional surgery for hepatic tumors. Hepatology. 1997; 26:1176-1181.
107. Shukla A, Giri S. Portal Vein Thrombosis in Cirrhosis. J Clin Exp Hepatol. 2022; 12:965-979.
108. Heo S, Lee SS, Choi SH, Kim DW, Park HJ, Kim SY, Lee SJ, Kim KM, Shin YM. CT Rule-in and Rule-out Criteria for Clinically Significant Portal Hypertension in Chronic Liver Disease. Radiology. 2023; 309:e231208.
109. Tu R, Xia LP, Yu AL, Wu L. Assessment of hepatic functional reserve by cirrhosis grading and liver volume measurement using CT. World J Gastroenterol. 2007; 13:3956-3961.
110. Son JH, Lee SS, Lee Y, Kang BK, Sung YS, Jo S, Yu E. Assessment of liver fibrosis severity using computed tomography-based liver and spleen volumetric indices in patients with chronic liver disease. Eur Radiol. 2020; 30:3486-3496.
111. Yan C, Han X, Liang X, Jia J, Xu Y, Zhao L. Non-invasive evaluation of esophageal varices in patients with liver cirrhosis using low-dose splenic perfusion CT. Eur J Radiol. 2022; 152:110326.
112. Romero-Cristóbal M, Clemente-Sánchez A, Ramón E, *et al*. CT-derived liver and spleen volume accurately diagnose clinically significant portal hypertension in patients with hepatocellular carcinoma. JHEP Rep. 2023; 5:100645.
113. Bak S, Kim JE, Bae K, Cho JM, Choi HC, Park MJ, Choi HY, Shin HS, Lee SM, Kim HO. Quantification of liver extracellular volume using dual-energy CT: utility for prediction of liver-related events in cirrhosis. Eur Radiol. 2020; 30:5317-5326.
114. Morita K, Nishie A, Ushijima Y, Takayama Y, Fujita N, Kubo Y, Ishimatsu K, Yoshizumi T, Maehara J, Ishigami K. Noninvasive assessment of liver fibrosis by dual-layer spectral detector CT. Eur J Radiol. 2021; 136:109575.
115. Varenika V, Fu Y, Maher JJ, Gao D, Kakar S, Cabarrus MC, Yeh BM. Hepatic fibrosis: evaluation with semiquantitative contrast-enhanced CT. Radiology. 2013; 266:151-158.
116. Nagayama Y, Kato Y, Inoue T, Nakaura T, Oda S, Kidoh M, Ikeda O, Hirai T. Liver fibrosis assessment with multiphasic dual-energy CT: diagnostic performance of iodine uptake parameters. Eur Radiol. 2021; 31:5779-5790.
117. Barr RG, Wilson SR, Rubens D, Garcia-Tsao G, Ferraioli G. Update to the Society of Radiologists in Ultrasound Liver Elastography Consensus Statement. Radiology. 2020; 296:263-274.
118. Duan T, Jiang HY, Ling WW, Song B. Noninvasive imaging of hepatic dysfunction: A state-of-the-art review. World J Gastroenterol. 2022; 28:1625-1640.
119. Sande JA, Verjee S, Vinayak S, Amersi F, Ghesani M. Ultrasound shear wave elastography and liver fibrosis: A Prospective Multicenter Study. World J Hepatol. 2017; 9:38-47.
120. Nguyen-Khac E, Thiele M, Voican C, *et al*. Non-invasive diagnosis of liver fibrosis in patients with alcohol-related liver disease by transient elastography: an individual patient data meta-analysis. Lancet Gastroenterol Hepatol. 2018; 3:614-625.
121. Selvaraj EA, Mózes FE, Jayaswal ANA, *et al*. Diagnostic accuracy of elastography and magnetic resonance imaging in patients with NAFLD: A systematic review and meta-analysis. J Hepatol. 2021; 75:770-785.
122. Berzigotti A, Seijo S, Arena U, Abraldes JG, Vizzutti F, García-Pagán JC, Pinzani M, Bosch J. Elastography, spleen size, and platelet count identify portal hypertension in patients with compensated cirrhosis. Gastroenterology. 2013; 144:102-111.e101.
123. Berzigotti A. Non-invasive evaluation of portal hypertension using ultrasound elastography. J Hepatol. 2017; 67:399-411.
124. Long H, Zhong X, Su L, Huang T, Duan Y, Ke W, Xie X, Lin M. Liver Stiffness Measured by Two-Dimensional Shear Wave Elastography for Predicting

Symptomatic Post-hepatectomy Liver Failure in Patients with Hepatocellular Carcinoma. Ann Surg Oncol. 2022; 29:327-336.
125. Cheng GW, Fang Y, Xue LY, Zhang Y, Xie XY, Qiao XH, Li XQ, Guo J, Ding H. Nomogram based on liver stiffness and spleen area with ultrasound for posthepatectomy liver failure: A multicenter study. World J Gastroenterol. 2024; 30:3314-3325.
126. Shastri M, Kulkarni S, Patell R, Jasdanwala S. Portal vein Doppler: a tool for non-invasive prediction of esophageal varices in cirrhosis. J Clin Diagn Res. 2014; 8:MC12-15.
127. Elkenawy YN, Elarabawy RA, Ahmed LM, Elsawy AA. Portal vein flow velocity as a possible fast noninvasive screening tool for esophageal varices in cirrhotic patients. JGH Open. 2020; 4:589-594.
128. Evrimler S, Swensson JK, Are VS, Tirkes T, Vuppalanchi R, Akisik F. Quantitative assessment of disease severity of primary sclerosing cholangitis with T1 mapping and extracellular volume imaging. Abdom Radiol (NY). 2021; 46:2433-2443.
129. Jhaveri KS, Hosseini-Nik H, Sadoughi N, Janssen H, Feld JJ, Fischer S, Menezes R, Cheung AC. The development and validation of magnetic resonance elastography for fibrosis staging in primary sclerosing cholangitis. Eur Radiol. 2019; 29:1039-1047.
130. Tafur M, Cheung A, Menezes RJ, Feld J, Janssen H, Hirschfield GM, Jhaveri KS. Risk stratification in primary sclerosing cholangitis: comparison of biliary stricture severity on MRCP versus liver stiffness by MR elastography and vibration-controlled transient elastography. Eur Radiol. 2020; 30:3735-3747.
131. Aleksakhina SN, Imyanitov EN. Cancer Therapy Guided by Mutation Tests: Current Status and Perspectives. Int J Mol Sci. 2021; 22:10931.
132. Tan AC, Tan DSW. Targeted Therapies for Lung Cancer Patients With Oncogenic Driver Molecular Alterations. J Clin Oncol. 2022; 40:611-625.
133. Casolino R, Beer PA, Chakravarty D, Davis MB, Malapelle U, Mazzarella L, Normanno N, Pauli C, Subbiah V, Turnbull C, Westphalen CB, Biankin AV. Interpreting and integrating genomic tests results in clinical cancer care: Overview and practical guidance. CA Cancer J Clin. 2024; 74:264-285.
134. Tsilimigras DI, Kurzrock R, Pawlik TM. Molecular Testing and Targeted Therapies in Hepatobiliary Cancers: A Review. JAMA Surg. 2025; 160:576-585.

Received February 2, 2026; Revised March 13, 2026; Accepted March 20, 2026.

**Address correspondence to:*
Jiwei Huang and Haichuan Wang, Division of Liver Surgery, Department of General Surgery, West China Hospital, Sichuan University, #37 Guoxue Alley, Wuhou District, Chengdu 610041, Sichuan, China.
E-mail: huangjiwei@wchscu.cn (JW); haichuan.wang@wchscu.edu.cn (HW)

Released online in J-STAGE as advance publication March 25, 2026.